Features of Structure Formation and Electrophysical Properties of Poly(vinylidene fluoride) Crystalline Ferroelectric Polymers

Valentin V. Kochervinskii,[1] Nina V. Kozlova,[1] Alexey Y. Khnykov,[1] Maxim A. Shcherbina,[1] Serghey N. Sulyanov,[2] Kirill A. Dembo[2]

[1]*Karpov Institute of Physical Chemistry, 103064 Vorontsovo Pole 10, Moscow, Russia*
[2]*Institute of Crystallography, Russian Academy of Sciences, 119333 Leninskii Prospekt 59, Moscow, Russia*

Received 17 July 2008; accepted 30 June 2009
DOI 10.1002/app.31044
Published online 10 December 2009 in Wiley InterScience (www.interscience.wiley.com).

ABSTRACT: The influence of intramolecular dipole–dipole interaction changes on structure formation peculiarities and some electrophysical properties were investigated with example of copolymers of vinylidene fluoride with tetrafluoroethylene and hexafluoropropylene with different compositions. The decrease of such dipole–dipole interactions in vinylidene fluoride/tetrafluoroethylene copolymers leads to an increase of the *a* and *b* parameters of the ferroelectric phase lattice and were accompanied by a shift of the Curie point to lower temperatures. The presence of peak-halo at angles near $2\theta = 18^\circ$ were attributed to a paraelectric phase localized in the interfacial domains at the crystal–amorphous phase boundaries. Similar peak-halos for vinylidene fluoride/hexafluoropropylene copolymers crystallizing into the nonpolar α phase were associated with the presence of an antiferroelectric phase formed by the chains in the planar zigzag conformation. The temperature range where dielectric anomalies were detected was characterized by conformational changes at which the decrease in planar zigzag conformation isomers took place.
 J Appl Polym Sci 116: 695–707, 2010

Key words: crystallization; ferroelectricity; fluoropolymers; phase behavior; structure

INTRODUCTION

Poly(vinylidene fluoride) (PVDF) and its copolymers are of interest because of the discovery of ferroelectricity and strong piezoelectricity and pyroelectricity.[1–4] These crystalline polymers form at least four crystallographic modifications: α, α_p, β, and γ.[5–14] The α and α_p forms are characterized by a $TGTG^-$ chain conformation but have nonpolar and polar cells, respectively. The polar β and γ phases have planar zigzag and $T_3GT_3G^-$ conformations, respectively. The crystallization of PVDF from the melt at moderate pressures is accompanied by the formation of a polymorphous α phase, which is converted to the polar α_p form by the action of a high electric field.[15–19] The polar β form usually forms under the action of the uniaxial drawing of PVDF isotropic films[19] or by nonisotermic crystallization from the melt at a high rate of cooling.[20–22] If the supercooling of the melt is low, the γ phase forms.[19,23]

Some peculiarities have been detected during PVDF crystallization from solutions.[24–41] For example, the ratio of the α and γ phases was found to be the function of water additive conductivity during the crystallization of PVDF in a solution of monochlorbenzene and dimethylformamide (DMFA; with the addition of 0.5% of water). The increase in the γ phase can be initiated by the addition of KBr to dimethylacetamide.[27] The introduction of LiCl into this solvent will promote the crystallization of the β and γ modifications in the mixture.[27] The type of polymorphous modification of PVDF during the crystallization from dimethyl sulfoxide is determined by the type of substrate.[28] The α phase arises on Teflon, steel, and aluminum (with oxide film on the surface), but the polar β phase preferentially forms on Cu, Si, and Au.[28] The type of crystalline modification for PVDF solution in methylethylketone can depend on the molecular weight of the chain.[29] The conclusion was obtained with samples with the equal contents of HHTT defects able to affect the polymorphism.[30–32] A decrease in the film-forming temperature (in a solution of dimethylacetamide) from 170 to 60°C changes the polymorphous modification from γ to β.[33,34] The precipitation temperature change has an affect on the surface roughness of the forming film.[35] It cannot be ignored that the gelling stage has an important part in this process.[36,37] The

Correspondence to: V. V. Kochervinskii (kochval@mail.ru).
Contract grant sponsor: Russian Foundation for Basic Research; contract grant numbers: 07-03-01034, 02445.11.7141.

purity of surface on which the film precipitates is one more factor that affects the polymorphous modification type. This has been checked for PVDF solutions in dimethyl sulfoxide[38] and in an acetone/DMFA mixture.[39] The presence of bound water molecules in the solution is important for the formation of the crystal structure, too.[40,41] This conclusion can be qualitatively confirmed by the characteristics of the equilibrium swelling of PVDF, too.[42]

The influence of intramolecular dipole–dipole interactions on the structure and electrophysical properties of copolymers was investigated in this study with an example of two vinylidene fluoride (VDF) copolymers. VDF copolymers with tetrafluoroethylene (TFE) and hexafluoropropylene (HFP) of different compositions were used. Both comonomers were nonpolar; therefore, the increase of their fractions in the statistic copolymer caused a decrease of intrachain dipole–dipole interactions. The TFE replacement by HFP allowed us to simultaneously trace the role of steric factors in the structure forming in copolymers of the same composition. The VDF/TFE copolymers [and VDF/trifluoroethylene (TrFE)] crystallized from the melt at a moderate pressures into a ferroelectric β phase.[6] This was true only for copolymers where the fraction of the named comonomers was greater then the critical value. For instance, crystallization into the β phase of the VDF/TrFE copolymers from the melt was observed at compositions of 83 : 17[6] or 88 : 12.[43] The crystallization of the VDF/TFE copolymers into the isotropic polar β phase was observed at critical composition of 93 : 7.[6]

The structure formation of the VDF/TFE copolymer of 94 : 6 composition near a critical one (during the crystallization from the melt) was investigated in more detail in this study. The pressure decrease in the melt promoted the appearance of nonpolar α-phase crystals along with the polar β-phase crystals. The crystallization of the mentioned copolymer with the formation of films from solutions in different solvents occurred in the mixture of the polar β and γ phases. The decrease of the intramolecular dipole–dipole interactions at the TFE fraction augmentation in the discussed copolymer leads to the expansion of the lattice in the *a* and *b* directions. A similar tendency (although to a smaller degree) was detected at the increase of the HFP fraction in the VDF/HFP copolymers, which crystallized in the nonpolar α phase. The steric hindrances of HFP groups in these copolymers lead to decreases in the crystallinity and crystal dimensions and to a rise in the average interchain spacing in the amorphous phase. The X-ray diffraction patterns of all of the investigated copolymers contained a peak-halo in the area near $2\theta \approx 18^\circ$. This was attributed to the presence of a paraelectric or antiferroelectric phase in the obtained films.

EXPERIMENTAL

Samples

The VDF homopolymer (F2E, Russia) and its copolymers with TFE and HFP were studied. All of the polymers were characterized by ^{19}F-NMR to determine the molar proportion of comonomers and to evaluate the number of chemical defects of HHTT type.[44–46] Two VDF/TFE copolymers were explored. For the first one, the molar fraction of TFE was about 6%, and the number of HHTT defects was 4.5 mol %.[44] The other one from the set had 29% TFE, and the number of HHTT defects was 2.5 mol %. A part of TFE had a dyad form.[45] Two other VDF/HFP copolymers had HFP fractions of 7 and 14 mol %.[46]

The samples of the isotropic PVDF films and VDF/TFE copolymers were prepared by two methods: crystallization from the melt and from the solution. By the first method, the polymer was melted, and the films were formed under a pressure of 15 MPa. Cooling conditions were varied. The films of the VDF/TFE (94 : 6) copolymer were crystallized at atmospheric pressure, too. Acetone, DMFA, or their mixture with ethyl acetate (EAC) were used as solvents. The polymer concentration was 8–10 wt %. The films were dried *in vacuo* to a constant weight after the completion of the formation process. The films of the VDF/HFP copolymers were prepared by extrusion.

Methods

Wide-angle X-ray scattering (WAXS) was performed with an X-ray diffractometer KARD-6 with a two-dimensional area detector and a graphite monochromator.[47] Cu Kα radiation (wavelength = 1.542 Å) was used. The diffraction peaks were analyzed by profile fitting. The crystal size (lc) was estimated with the Scherrer formula:

$$l_c = \frac{0.9k\lambda}{\cos\theta\sqrt{\beta^2 - \beta_r^2}} \quad (1)$$

where λ is the wavelength, k is the diffraction order, β is the full width at half-maximum (fwhm) for the sample measured, and β_r is the fwhm for the instrumental resolution function. The stack packing of the lamellar crystals was studied by small-angle X-ray scattering. The measurements were made on an AMUR-K (Shubnikov Institute of Crystallography, Moscow, Russia) diffractometer with a linear position-sensitive detector. A slit collimation was used, and the standard desmearing procedure was performed. The data was performed in *I–s* coordinates, where I is the intensity and the scattering vector (s) was

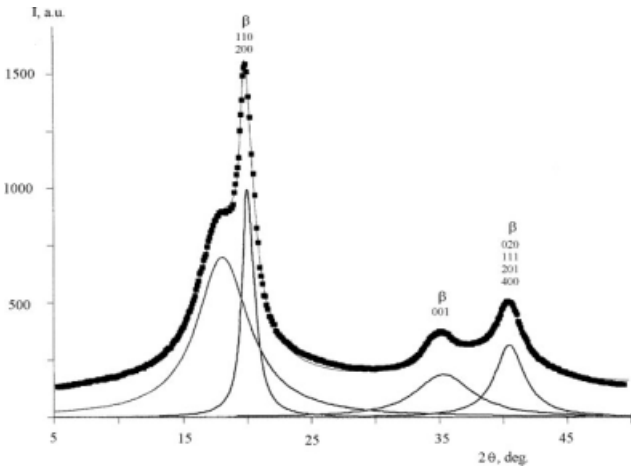

Figure 1 Diffraction patterns of an isotropic film of VDF/TFE (94 : 6) produced from the melt by nonisothermal crystallization under 15 MPa of pressure with quenching into water at room temperature.

$$s = 4\pi \frac{\sin\theta}{\lambda}$$

The large period (L) was determined as follows:

$$L = 2\pi/s_{\max}$$

where $s_{\max}$ is the scattering vector corresponding to the maximum intensity. The particles' micrometer size was observed by small-angle polarized light scattering. The average radius (R) of the spherulites was obtained at the scattering pattern (between crossed polarizers) from a ratio: [48]

$$\frac{4\pi R}{\lambda}\frac{\sin\theta_m}{2} = 4.1 \qquad (2)$$

where λ is the wavelength in the medium and θ_m is the radial scattering angle corresponding to the maximum intensity. To measure the switching of polarization, the aluminum electrodes (100 nm thick) were evaporated onto the samples. The Curie transitions were registered by the temperature dependence of the dielectric permittivity (frequency = 1 kHz) at a heating rate of 2°/min. The currents of switching were measured by means of the Sawyer–Tower method.

RESULTS

We will analyze the peculiarities of the forming structure, which were not discussed earlier. In particular, we give great attention to the structure and identification of the nonordered phase in these polymers. As noted previously, the crystallization with a copolymer composition of 93 : 7 from the melt under moderate pressure leads to the formation of the polar β modification.[6,19] It is known that the external pressure toward PVDF favors the formation of the polar β phase.[7,49–51] So it was interesting to answer the following question: does the pressure at crystallization from the melt influence the structure of the VDF/TFE copolymer if its proportion (94 : 6) is close to critical (93 : 7[6])?

Figures 1 and 2 show the X-ray diffraction from films of the copolymer crystallized at pressures of 15 and 0.1 MPa. It was clear that in the first case, the ferroelectric β phase was formed, whereas the second one was a mixture of the α and β phases. This conclusion was confirmed by the data of IR spectroscopy (Fig. 3). The spectra showed bands of the conformations of $TGTG^-$ (α phase) and a planar zigzag (β phase). It was possible to compare the structural characteristics of the α phase formed in

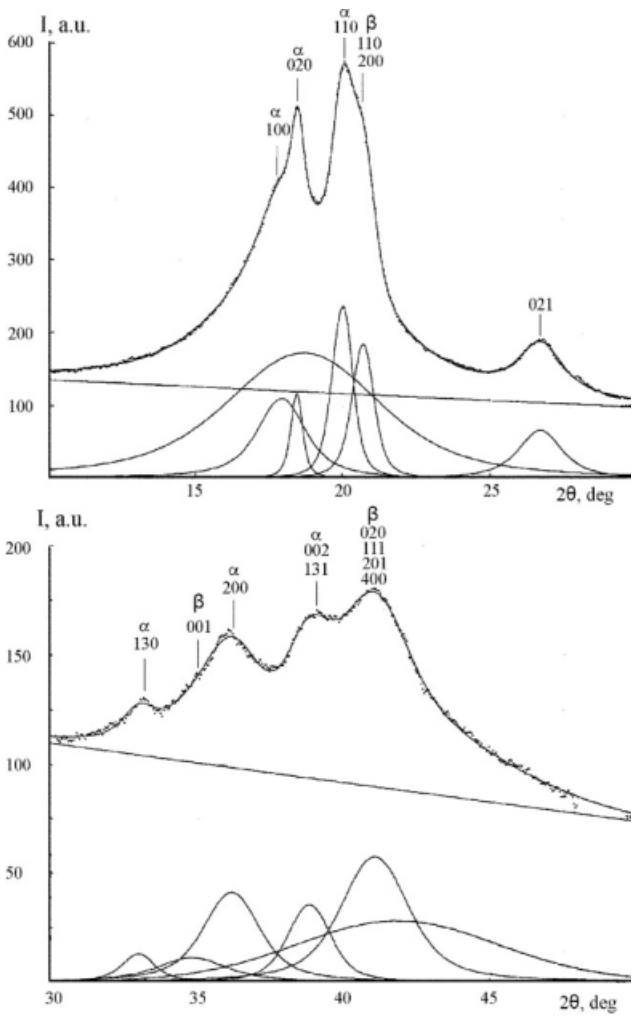

Figure 2 Diffraction patterns of an isotropic film of VDF/TFE (94 : 6) produced from the melt by nonisothermal crystallization under atmospheric pressure.

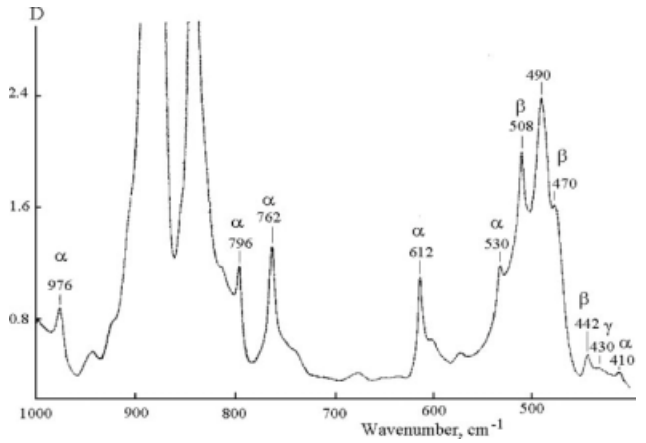

Figure 3 IR spectroscopy data of an isotropic film of VDF/TFE (94 : 6) produced from the melt by nonisothermal crystallization under atmospheric pressure.

the VDF/TFE copolymer (Fig. 2) to that of the homopolymer (Fig. 4). The comparison of X-ray patterns showed that in the former case, the number of peaks (especially at wider angles) was lower and its fwhm was substantially larger. This meant that the α phase of the copolymer was less perfect. Galperin and Kosmyini[52] showed that there are two types of α phases with different ordering. These can be realized by changing the parameters of a cell.

Let us consider that the α phase in the copolymer is also described by a monoclinic cell as a homopolymer. In this case, the parameters of the cell for the homopolymer are $a = 0.497$ nm, $b = 0.963$ nm, $c = 0.463$ nm, and $\beta = 90.5°$. These corresponded to the previous data.[9] These parameters in the copolymer were the following: $a = 0.501$ nm, $b = 0.968$ nm, $c = 0.464$ nm, and $\beta = 98°$. In comparison with the homopolymer, the copolymer had a small increase in the cell size in the a and b directions and a significant increase in the β angle. It was interesting to compare the WAXS and spectroscopic data for the β-phase fraction [$F(\beta)$] in its mixture with the α phase. According to WAXS, only about one third of crystals is formed in polar β modification (Table I). Otherwise, according to IR spectroscopy, the relation between the intensities of the 530- and 508-cm^{-1} bands (the last one characterizes the planar zigzag conformation of the β phase) gave $F(\beta) = 0.84$. The two methods showed a substantial difference between the values of $F(\beta)$.

The contradiction disappears if we propose that the absorption band of 508 cm^{-1} was responsible for the planar zigzag conformation both in the crystal and amorphous phases.[19] This means that the samples of the copolymer had an enhanced content of planar zigzag conformation in the amorphous phase. These fragments could be placed on the crystal boundaries and could be included in the α-phase crystals (of the $TGTG^-$ conformation) as conformational defects. The last suggestion explains the small size of the domains of coherent scattering for the α-phase crystals. These structure peculiarities and different cell parameters can lead to unusual properties in these copolymers. These copolymers had a high sensitivity to external forces, for example, this phase transformation to the β phase at heating.[53] Similar α → β transformation took place under irradiation.[54]

The lamellar crystals in this copolymer formed a supramolecular structure of spherulite type. An inherent four-clover picture of H_v (at crossed polarizers) light scattering had a strong intensity that was typical for spherulites of the α phase, where the difference between the radial and tangential polarization of a particle was high. The spherulite size (Rsph) obtained by eq. (2) was 4–8 μm for different samples. We observed H_v scattering corresponding to a bimodal size distribution of spherulites in some tests. Low-intensity scattering at the wider angles was observed from the small

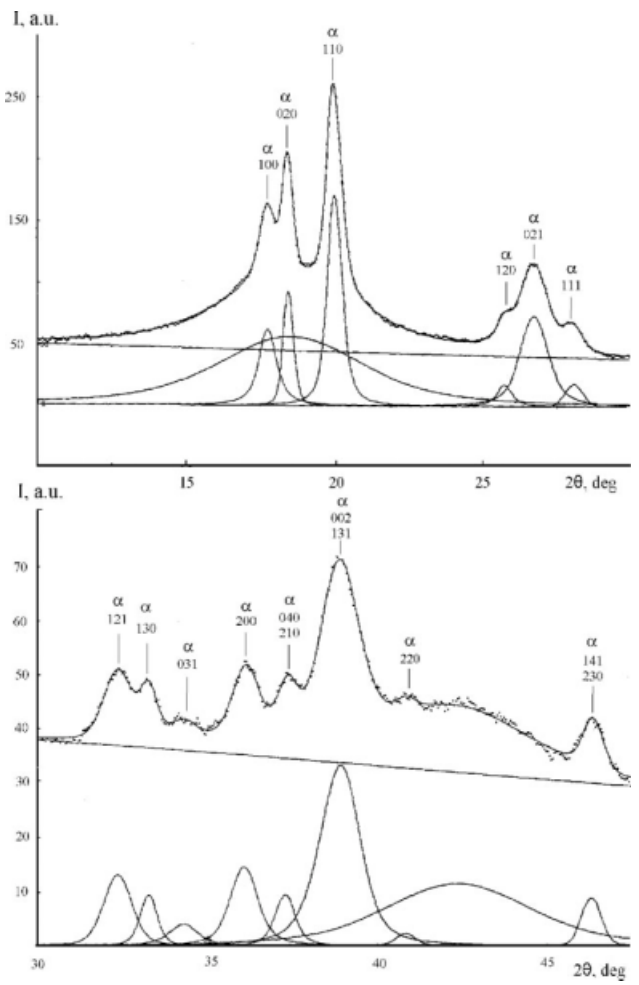

Figure 4 Diffraction patterns of an isotropic PVDF film crystallized isothermally at 150°C from the melt.

TABLE I
Structural Parameters of Initial Isotropic Films of VDF/TFE and VDF/HFP Copolymers Formed with Different Methods

	Copolymer composition							
	94 : 6 VDF/TFE					71 : 29 VDF/TFE	93 : 7 VDF/HFP	86 : 14 VDF/HFP
	From solution in DMFA	From solution in DMFA and EAC	From solution in acetone	Quenched from the melt at 15 MPa	Quenched from the melt 0.1 at MPa	From solution in acetone	Extrusion	Extrusion
L (nm)	11.6	12.8	—	13.5	11.8	30.0	10.5	16.0
l_{001}^{β} (nm)	3.3	2.8	2.1	3.9	2.8	5.9	—	—
l_{002}^{α} (nm)	—	—	—	—	4.9	—	4.0	1.8
l_a (nm)	8.3	10.0	—	9.6	8.0	24.1	6.5	14.2
$l_{110,200}^{\beta}$ (nm)	5.7	6.3	6.5	7.9	9.5	8.8	—	—
l_{110}^{α} (nm)	—	—	—	—	10.5	—	10.7	6.8
Rsph (mcm)	2.6	—	—	1.4	6.0	—	—	—
$F(\beta)$	0.73	0.77	0.68	1.0	0.32	1.0	—	—
ϕ_L	0.33	0.34	—	0.30	0.33	0.18	0.38	0.11
ϕ_1	0.44	0.38	0.29	0.46	0.38	0.34	0.21	0.17
ϕ_2	0.56	0.47	0.85	1.0	0.46	0.83	0.43	0.38
ϕ_p	0.20	0.18	0.55	0.46	0.32	0.59	0.51	0.55
l_p (nm)	2.8	2.8	1.3	3.5	4.1	2.3	2.5	2.6

l is the crystal size in the direction designated by the subscript belonging to the phase designated by superscript. l_a is the thickness of amorphous layer between the neighbouring crystals along their c-axis.

spherulites (~1 μm), which were characterized by the small value of their intrinsic birefringence.

The nature of the amorphous phase for the VDF/TFE copolymer crystallized in the β phase (Fig. 1) is discussed separately. It could be associated with the peak-halo around the angle of 18°, as is common for VDF copolymers with TrFE.[55–58] The peak 100 (Fig. 4) was within this angular region, whereas the amorphous halo shifted to wider angles. A specific feature of the peak-halo of VDF/TFE was that its fwhm was about two times lower than the halo for PVDF. The crystallinity of the VDF/TFE (94 : 6) isotropic film was 46% according to WAXS measurements. It was interesting to observe the existence of this peak-halo for other methods of crystallization of this copolymer. We used crystallization from solution, which allowed us to obtain different polymorphic modifications.[33–41,59–62] The change in the solvent affinity can influence on polymer morphology.[63,64] Three solvents were used: DMFA with its good affinity to PVDF, acetone, and a mixture of DMFA and EAC (a bad solvent). The X-ray data showed that crystallization of VDF/TFE (94 : 6) in all cases lead to a mixture of the β and γ phases. It was shown in the example of films formed from DMFA solution (Fig. 5) because there were peaks of both phases on the diffractograms. The ratios of the β and γ modifications and their crystallinity were calculated for initial films of three types.

Table I illustrates that the aggravation of the solvent affinity lead to some decrease in the crystallinity, whereas the proportion of the β and γ phases remained

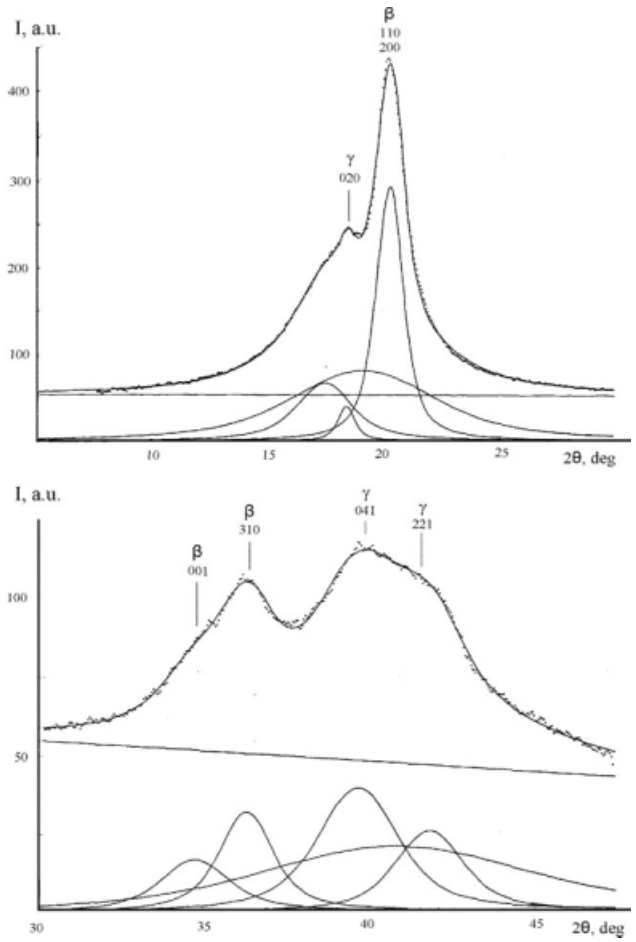

Figure 5 Diffraction patterns of an isotropic film of VDF/TFE (94 : 6) produced from a solution of DMFA.

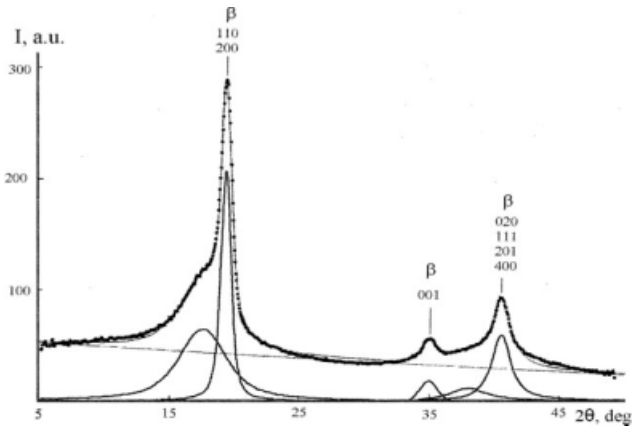

Figure 6 Diffraction patterns of an isotropic film of VDF/TFE (71 : 29) produced from an acetone solution.

the same. For this method of crystallization, the diffraction pattern was also characterized by the mentioned peak-halo (Fig. 5). At the same time, $F(\beta)$ (in the mixture with the γ modification) did not depend on the solvent type (Table I). The lamellar stacking of crystals was similar for all of the three solvents because L was the same (Tabl.1). However, the secondary structures of

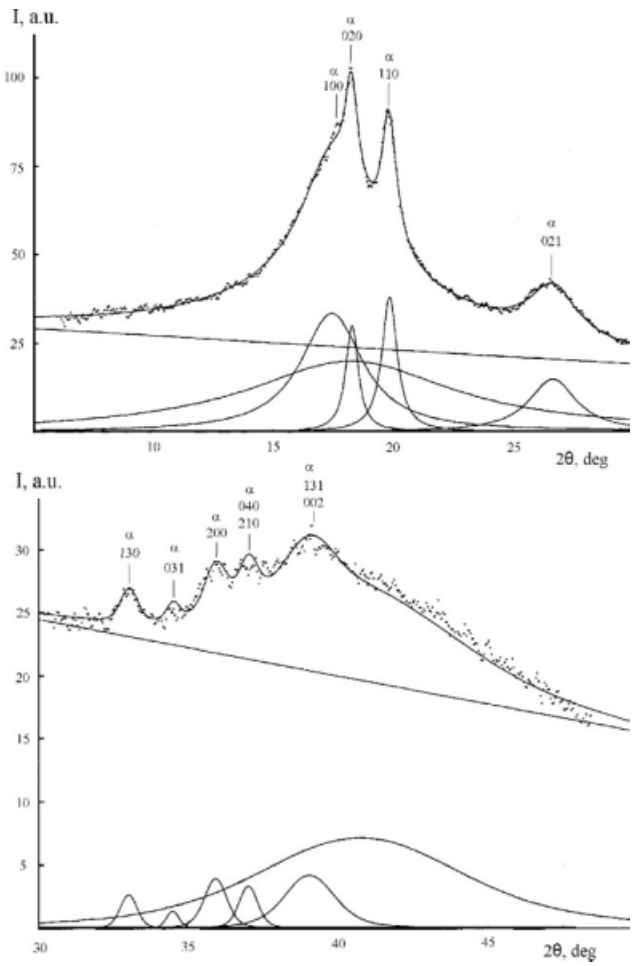

Figure 7 Diffraction patterns of an extruded film of VDF/HFP (93 : 7).

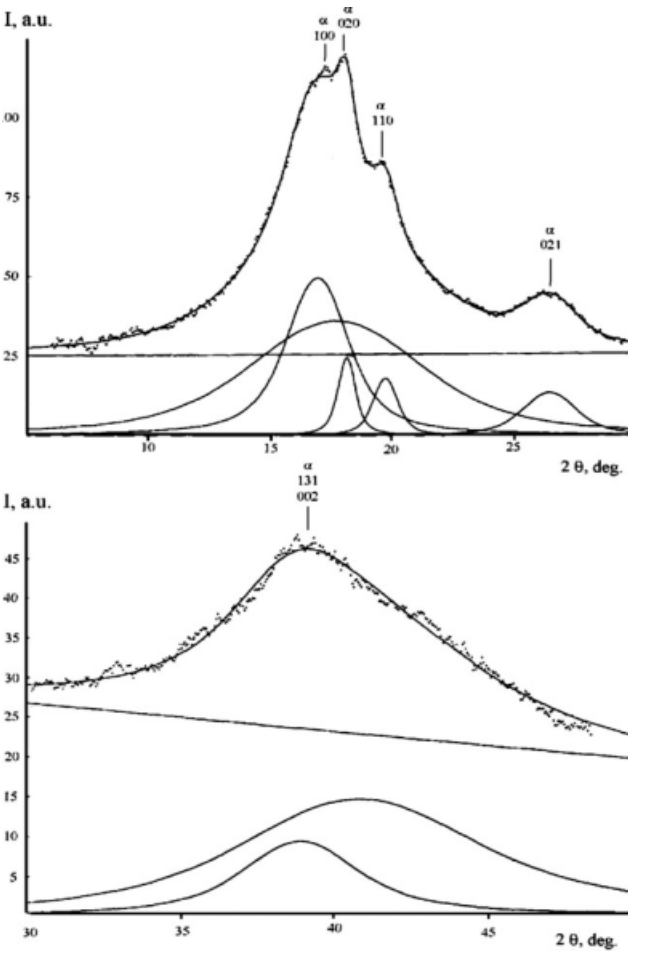

Figure 8 Diffraction patterns of an extruded film of VDF/HFP (86 : 14).

micrometer size were different according to small-angle polarized light scattering. The films crystallized from DMFA solution contained spherulites with 2–3-μm radii. Such structures were not found for the films prepared from DMFA+EAC or from acetone. The scattering intensity measured for the parallel polarizers was very low. In the first approximation, it may have been connected with the small difference between the crystals and the matrix refraction.[65]

Figure 6 shows that the increase in TFE in this copolymer up to 29 mol % lead to the formation of the ferroelectric β phase at crystallization from acetone. The peak-halo at angles $\sim 18^\circ$ is also present as well as in copolymer or 94/6 composition (Fig. 1) and in the copolymer VDF/TFE of 71 : 29 composition (Fig. 6). It was also observed in the 93 : 7 (Fig. 7) and 86 : 14 (Fig. 8) VDF/HFP copolymer compositions.

DISCUSSION

Copolymers of VDF and TFE

When the VDF/TFE copolymers were crystallized in the polar β phase, there should have been a

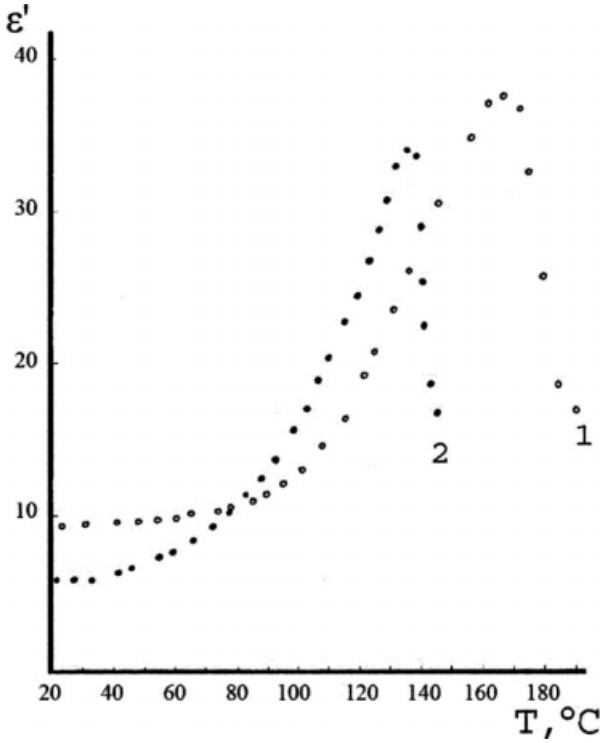

Figure 9 Temperature (T) dependence of the dielectric permittivity (1 kHz) for initial films of VDF/TFE: (1) 94 : 6 (crystallization by quenching from the melt) and (2) 71 : 29 (crystallization from an acetone solution).

ferroelectric–paraelectric transition that could be registrated by a dielectric anomaly. This transition can be seen in Figure 9, where the temperature dependence of the linear dielectric permittivity (ε′) for the VDF/TFE copolymers is shown. The ε′ anomaly in copolymer with 29 mol % TFE moved by 30° to lower temperatures. Figure 10 shows the field dependences of the switching currents in isotropic

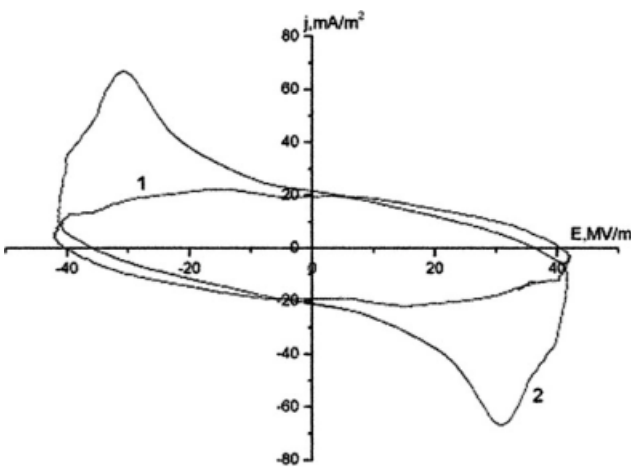

Figure 10 Field dependence of the switching current spontaneous polarization in isotropic films of VDF/TFE copolymers: (1) 94 : 6 and (2) 71 : 29 (temperature = 22°C, frequency = 50 Hz). E is the strength of electric field, j is the current density.

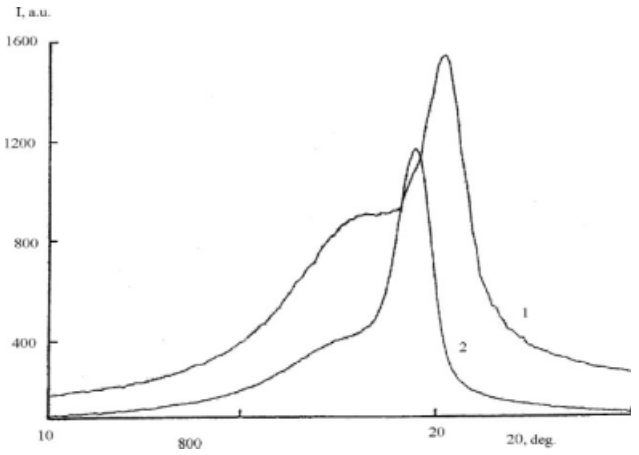

Figure 11 Comparison of the diffraction patterns for the intermolecular peaks of isotropic films of VDF/TFE copolymers: (1) 94 : 6 and (2) 71 : 29.

films of these copolymers. In copolymers with 29 mol % TFE, the coercive field was 30 MV/m. For the copolymer with a smaller fraction of TFE, this field was certainly higher because the switching of the spontaneous polarization was not found at the same field. This result agree with earlier data.[45] The X-ray patterns for these copolymers (Fig. 11) are also different. The increase of TFE fraction leads to a significant shift of the 110, 200 peaks to smaller angles. We obtained the following cell parameter values for the orthorhombic VDF/TFE copolymer (94 : 6): a = 0.865 nm, b = 0.499 nm, and c = 0.251 nm. The increase in the fraction of TFE up to 29 mol % leads to a decrease in the packing density along the a and b cell directions: a = 0.913 nm and b = 0.527 nm. This result agrees with ref. 6. It means that interchain potential played an important role in the ferroelectric–paraelectric transition and in the switching of spontaneous polarization.

The structure of the paraelectric phase in the VDF/TFE copolymer was not investigated previously. Earlier, it was investigated only for the VDF/TrFE copolymer.[66] In this study, we tried to fill this gap. In the region of $2\theta \approx 18°$ for the β phase of the VDF/TFE copolymers, there are not any peaks (Figs. 2 and 6), and the halo in this region for the copolymer of VDF/TrFE was connected with the amorphous phase.[55–58] As mentioned previously, the 100 peak of the nonpolar α modification was located in this region (Fig. 4).[19] From the other side, the main peak of the hexagonal paraelectric phase was located in this region, too.[66] So, for the VDF/TFE copolymers, which were crystallized in the polar modification, the peak-halo may have shown the presence of the paraelectric (antiferroelectric) phase.

The coexistence of ferroelectric and paraelectric phases at temperatures lower than the Curie point was noted before.[57,67] If the peak-halo refers to the

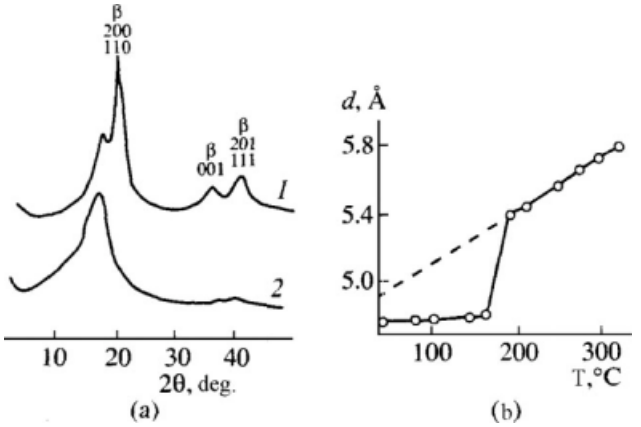

Figure 12 Temperature (T) dependence of (a) the X-ray diffraction and (b) interplane parameter d for a peak-halo in a film of a VDF/TFE copolymer (94 : 6): (1) 160 and (2) 184°C.[53]

paraelectric phase, it can be checked by temperature-dependent X-ray diffraction. It is shown in Figure 12.[53] At 160°C, the ferroelectric β-phase 110 and 200 main peak and a peak-halo are present. This means that a mixture of the ferroelectric and paraelectric crystals existed at this temperature. The peaks of the ferroelectric phase disappeared at temperatures higher than the melting temperature (Curie point), and only the peak-halo remained. A dielectric anomaly characterized for the ferroelectric–paraelectric transition was observed in the same temperature region (curve 1 in Fig. 9). It was interesting to follow where the domains of the paraelectric phase were localized. Some information about that could be extracted from the VDF/TFE 94 : 6 copolymer (see Fig. 12). The temperature dependence of the interplanar spacing (d-spacing) for the mentioned peak-halo is shown in Figure 12(b). A drastic increase in d was observed in the area of melting (the Curie point). Thus, the character of packing in the supposed paraelectric phase was controlled by the presence of crystals of the ferroelectric phase. On the other hand, these objects were crystallizing polymers, which had an interphase layer with an intermediate density of packing between the crystal and amorphous domains.[68] It was clear that the melting of the crystals leads to the destruction of these interphase layers. So, the mentioned paraelectric phase could have been localized exactly in these interphase layers.

If this hypothesis were true, the sizes of the paraelectric phase domain and the interphase layer should have been the same. The size of the suggested paraelectric domains (l_p) could be evaluated from the width of the peak-halo. Table I shows the l_p changes from 2 to 4 nm. The size of the interphase layer according to small-angle X-ray scattering was approximately the same.[69] There is a reason to conclude that the paraelectric phase domains are localized in the interphase layers between the crystal and amorphous phases. The following facts confirm this hypothesis. It is known that an intensive dynamic is observed for the paraelectric phase of these polymers.[66] Also, the exact interphase layers of PVDF were zones of realization of a high-amplitude cooperative processes of polymer segment reorientation.[69] Probably, antiferroelectric phase domains indicated in previous studies[3,71–73] also localized in these layers.

Copolymers of VDF and HFP

The discussed peak-halo was also present in the VDF/HFP copolymers (Figs. 7 and 8). These copolymers, as shown in Figures 4, 7, and 8 and in quality correspondence with data from the literature,[74–76] were crystallized in the α phase. In this phase, however, there is a peak 100 at an angle of $2\theta \approx 18°$. Nonetheless, we considered that in these copolymers, there was also the mentioned peak-halo. Really, the structural factor (F_{hkl}) values for the peaks 100, 020, and 110 were in the following relation: $F_{100} < F_{020} < F_{110}$.[19,77] However, the aforementioned relation of the integral intensity was disturbed for the VDF/HFP copolymers: $F_{100} > F_{020}$ and F_{110}. This means that the discussed peak-halo was probably localized in the mentioned angle region. Its angular position changed with increasing HFP fraction (Table II). The displacement of the peak-halo to lower angles (similar to ref. 78) means that the interchain packing density of the corresponding lattice decreased. We propose that this was the result of the incorporation of massive fragments of CF_3 to this lattice. These fragments could be incorporated also into the α-phase lattice. Table II shows that an increase in the fraction of HFP leads to displacement of all of the peaks to lower angles.

TABLE II
Peak Angles of the α Phase and Amorphous Halo of PVDF and P(VDF/HFP) Copolymers

Peak	PVDF[a]	93 : 7 P(VDF/HFP)	86 : 14 P(VDF/HFP)
100 (peak-halo)	17.77	17.44	17.01
020	18.43	18.29	18.23
110	20.01	19.85	19.84
021	26.74	26.67	26.63
130	33.27	33.00	—
200	36.11	35.90	—
040	37.34	36.99	—
Amorphous halo	18.7	18.2	17.8

[a] The sample was formed by isothermal crystallization at 150°C under 15 MPa of pressure.

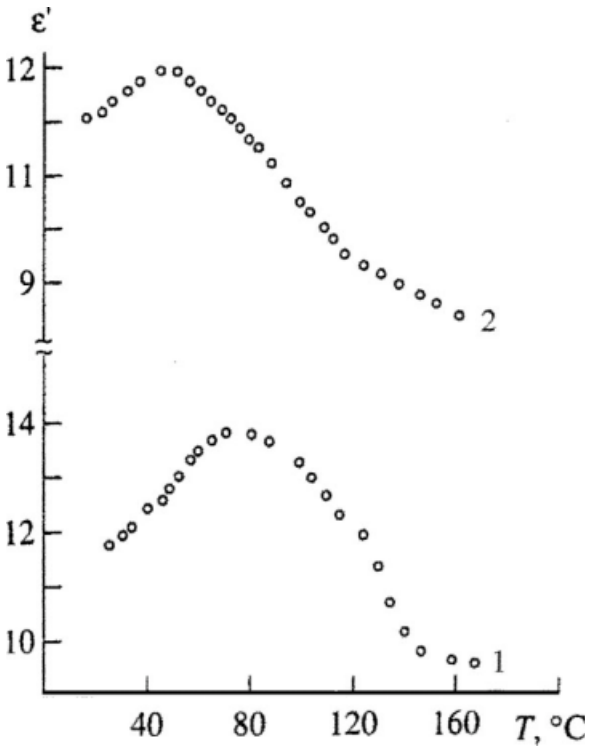

Figure 13 Temperature (T) dependence of the dielectric permittivity (1 kHz) for initial films of VDF/HFP: (1) 93 : 7 and (2) 86 : 14.

The parameters of cells for the adopted monoclinic lattice were the following: $a = 0.520$ nm, $b = 0.969$ nm, $c = 0.478$ nm, and $\beta = 105°$. A comparison with our data for the homopolymer showed that the incorporation of HFP fragments into the chain of PVDF leads to a decreased density of packing in the a and b axes and to an increase in the β angle from 90.5 to 105°. The incorporation of HFP groups into the α-phase lattice leads to decreases in the number of characteristic peaks and the sizes of the crystals in comparison to the homopolymer. A similar situation was observed for samples of polyethylene with different numbers of chain branching.[79] The of localization of the CF_3 fragments is maximal for nonordered phases because the angle positions of the amorphous halo and peak-halo changes significantly as the HFP fraction increases (Table II). An increase in the CF_3 concentration in the amorphous phase influenced the characteristics of mobility of the chain in these copolymers also.[80]

If one supposes that at room temperature, the VDF/HFP copolymers crystallizes into the α phase, an increase of temperature should not have resulted in an ε′ anomaly, as is typical for the ferroelectric–paraelectric phase transition. Nevertheless, the experiment do not confirm it. Figure 13 shows the temperature dependences of ε′ for both copolymers. An ε′ anomaly in the range 50–80°C indicates the ferroelectric phase transition, which is also confirmed by the differential scanning calorimetry data.[80] The temperature of this phase transition was approximately the same as that of the low-ordered ferroelectric phase (cooled phase), which is often observed in VDF/TrFE.[3,81] The mechanism of formation of this phase in our polymers was similar to the one observed in many amorphous nonorganic ferroelectrics.[82] The spontaneous polarization domains likely represented nanocrystals. As a result, the peaks from them were widened and were not registered by X-ray methods (Figs. 7 and 8).

IR spectroscopy indicates the presence of these domains due to the appearance of the absorption bands at 1280, 840, 470, and 442 cm^{-1}, which were found in the investigated copolymers. These bands, which are always observed in these polymers on crystallization in the ferroelectric phase,[1,2,19] corresponded to the planar zigzag conformations. Thus, the structure of the investigated copolymers at room temperature was characterized by the presence of a mixture of the α-phase crystals and nanocrystals of the polar β modification. Because the latter were formed by chain segments in planar zigzag conformation, the mentioned nanocrystals could generate the antiferroelectric phase, which may exist in the class of polymers studied.[3,74] The increase in the HFP fraction from 7 to 14% resulted in the growth of the polar β-phase fraction. Really, it is evident from Figure 14 that the increase in the HFP fraction from 7 to 14 mol % leads to an increase in the ratios of the optical densities of the absorption bands at 442 and 410 cm^{-1} (D_{442}/D_{410}) and at 470 and 410 cm^{-1} (D_{470}/D_{410}), where the bands at 442 and 470 cm^{-1} characterized chains with planar zigzag conformation and the band at 410 cm^{-1} characterized the $TGTG^-$ conformation α phase. On the other hand, it follows from Figures 7 and 8 that the mentioned HFP fraction increase in the copolymer results in the

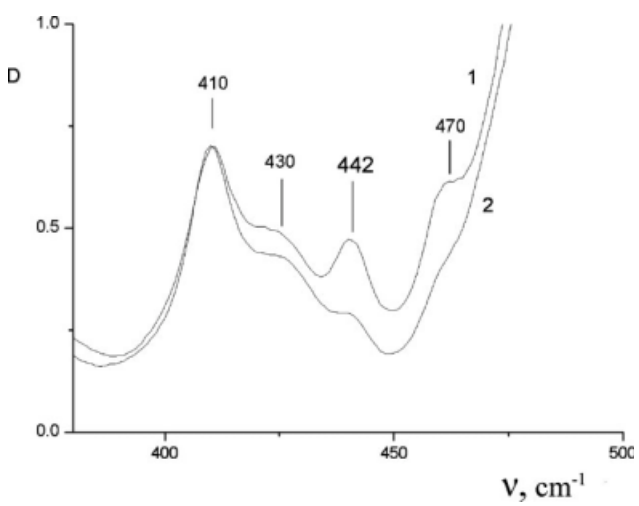

Figure 14 IR spectra of P(VDF/HFP) copolymers: (1) 86 : 14 and (2) 97 : 3.

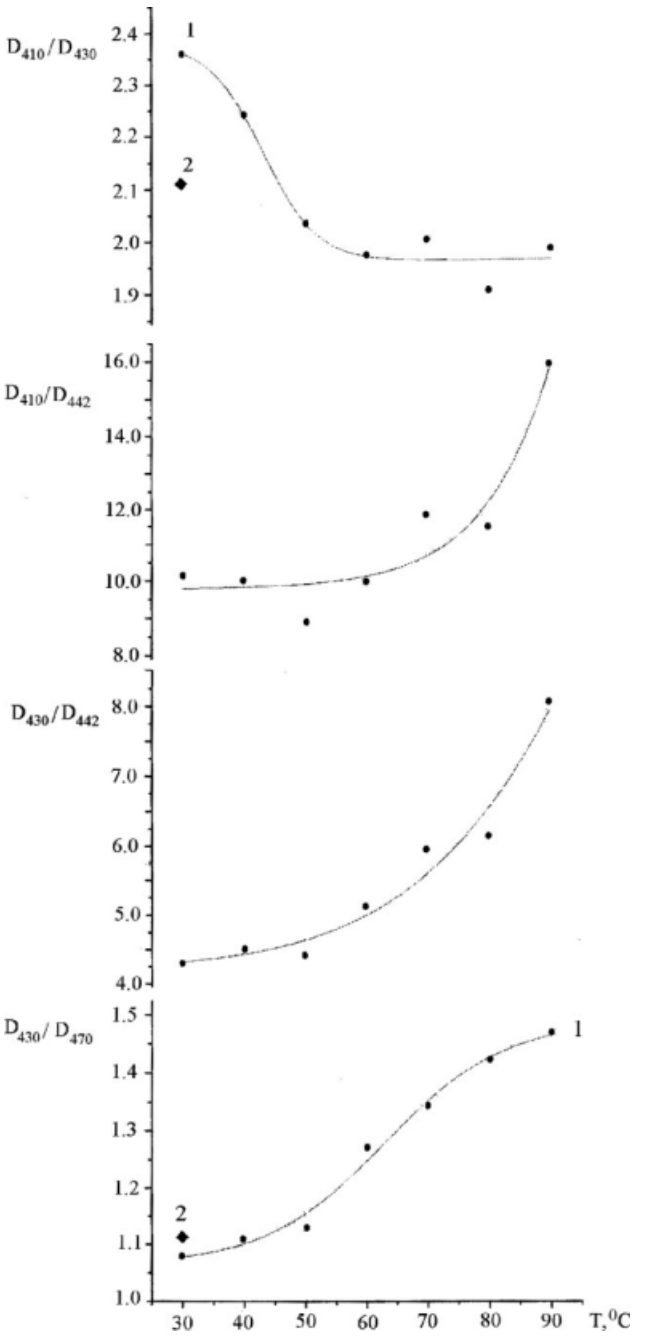

Figure 15 Temperature (T) dependence of the D ratios at some bands of the IR spectra of a P(VDF/HFP) 93 : 7 copolymer.

rise of the ratios $I_{p\text{-}h}/I_{020}$ and $I_{p\text{-}h}/I_{110}$, where $I_{p\text{-}h}$ is the integral intensity of the peak-halo and I_{020} and I_{110} are the integral intensities of the 020 and 110 peaks of the same α phase. Thus, mentioned correlation indicated that the peak-halo in the VDF/HFP copolymers should have been associated with the presence of chain segments in an anomalous planar zigzag conformation. Moreover, an unexpected conclusion followed from the considered data. All methods (including WAXS and differential scanning calorimetry) showed that the crystallinity in the VDF/HFP copolymer of 93 : 7 composition was noticeably higher. So, an increase in the crystal fraction of the nonpolar (α) phase suppresses the formation of the supposed antiferroelectric phase domains.

The transitions in this phase were determined from the temperature dependences of the IR spectra in the interval, where dielectric and thermal anomalies were observed. In particular, the bands at 410, 430, 442, and 470 cm^{-1} were analyzed. The first band characterized the $TGTG^-$ conformation (α phase), the second one characterized the $T_3GT_3G^-$ conformation (γ phase), and the two latter bands were responsible for the planar zigzag conformation (β phase).[3,6] Because the initial films were in a metastable (as-extruded) state and nonreversible changes in the texture and thickness were possible on heating, the spectral data were expressed as a ratio of the optical density (D) values of the conformation-sensitive absorption bands. The temperature dependences of such values are shown on Figures 15 and 16 for copolymers having ratios of 93 : 7 and 86 : 14, respectively, for their components. The following general regularities were noted for both of them. An increase in the D_{430}/D_{442} and D_{430}/D_{470} ratios (Fig. 15) with temperature for the copolymer with 7 mol % HFP was consistent with the conformation transitions such as $(\text{—TT—})_n \rightarrow (T_3GT_3G^-)$. On the other hand, an increase in the ratio D_{410}/D_{442} under the previous conditions pointed to

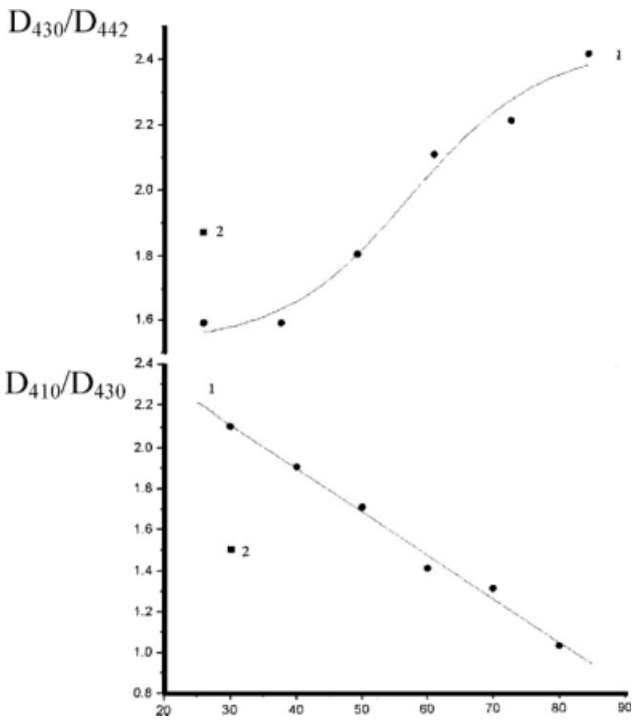

Figure 16 Temperature dependence of the D ratios at some bands of the IR spectra of a P(VDF/HFP) copolymer (86 : 14).

the transition $(\text{—TT})_n \rightarrow (\text{TGTG}^-)$. The former type of isomeric transformations was observed also in the VDF/HFP copolymer with an 86 : 14 component ratio (upper curve in Fig. 16). From Figures 15 and 16, it is clear that a decrease in the D_{410}/D_{430} ratio with increasing temperature was observed for both copolymers. This implied that the temperature increment caused the conformation transformations expressed by $(\text{TGTG}^-) \rightarrow (\text{T}_3\text{GT}_3\text{G}^-)$. This conclusion in some way correlates with the earlier mentioned data that high-temperature PVDF crystallization in the mixture of the α and γ phases always increased the fraction of the latter modification.[19] The aforementioned conformation rearrangements could also be registered by the analysis of the temperature dependence of the other absorption band's parameters. In particular, the temperature increase was accompanied by a noticeable widening of the absorption bands of the doublet of symmetric and antisymmetric stretching vibrations of methylene groups. This could be explained by the appearance of isomeric rearrangements because the frequencies of those bands for three various conformations were markedly different.[19]

It is necessary to underline the reversibility of the conformation changes discussed. The verification of this fact was accomplished by a comparison of parameters of selected bands before and after heating. The heating was accompanied by both reversible and nonreversible structural changes, even at temperatures much lower than the melting point. The latter are analyzed in Figures 15 and 16 by comparison of the optical band ratios at room temperature before (point 1) and after (point 2) the heating of the investigated films. A considerable decrease in the D_{410}/D_{430} ratio was observed. At the same time, a lack of coincidence could be seen between the virgin D ratios in the 7 mol % HFP copolymer (D_{430}/D_{470}, Fig. 15) and in the 14 mol % HFP copolymer (D_{442}/D_{410}, Fig. 16).

The analysis of X-ray patterns showed that the initial extruded film of the VDF/HFP copolymer of 93 : 7 composition is characterized by a certain orientation because the α-phase peak intensity depended on the azimuth angle (ϕ). The orientation function (f_c) was estimated through the off-orientation angle (γ) according to Hermans equation:

$$f_c = (\langle 3\cos^2\gamma\rangle - 1)/2 \tag{3}$$

The mean square ($\langle\cos^2\gamma\rangle$) was calculated as follows:

$$\langle\cos^2\gamma\rangle = \frac{\int_0^{\pi/2} \cos^2\phi \times \sin\phi \times I(\phi)d\phi}{\int_0^{\pi/2} \sin\phi \times I(\phi)d\phi} \tag{4}$$

Calculation according to eqs. (3) and (4) for the 020 and 110 peaks gave $f_c = 0.39$.

Azimuth scanning showed that the peaks being considered could be expressed as the sum of two components: isotropic and anisotropic. Evaluations showed that the fraction of the latter is equal to 8%. The orientation state was estimated in detail with the azimuth dependence of the integral intensity of some

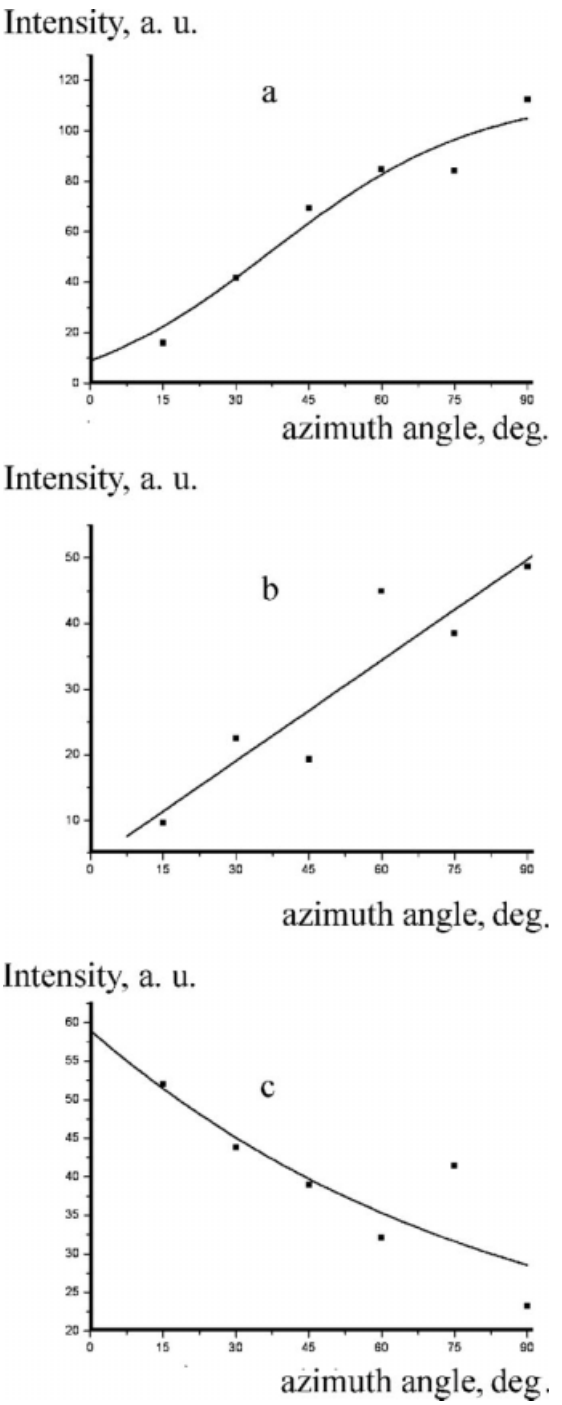

Figure 17 Azimuth dependence of the integral intensity of (a) the peak-halo, (b) peak 002, and (c) peak 110 in extruded films of a P(VDF/HFP) copolymer (93 : 7).

peaks of X-ray patterns during scanning from 0° (equator) to 90° (meridian) with steps of 15°. These data are exhibited in Figure 17. The 110 peak had a maximum intensity on the equator, whereas the 002 peak had a maximum intensity on the meridian. These facts point to the preferential orientation of the crystal *c* axis with regard to the extrusion direction. It was surprising that the integral intensity of the peak-halo behaved the same way as the 002 peak during the changing of ϕ. We could explain this only by supposing that the peak-halo belonged to areas of the interfacial boundary crystal–amorphous phase with an intermediate form of order. These domains must have been characterized by preferential orientation with regard to the extrusion direction as the core crystal.

The presence of the mentioned orientation was revealed also by IR spectroscopy because the absorption bands were characterized by dichroism. This belonged not only to the α-phase bands but also to the polar β-phase bands. The latter implied that the supposed antiferroelectric phase really could be localized in the interfacial regions. All of this means that marked changes in the *D* ratios of the conformation-sensitive absorption bands after the heating cycle were associated with a partial orientation loss because the heating was free (without the fixing of the film ends). The orientation loss was initiated just by the appearance of mobility in the domains of the supposed antiferroelectric phase. For the copolymer of 93 : 7 composition, which crystallized in the α phase, it is necessary to take into account the appearance of mobility being fixed by the dielectric method in crystal.[80]

The paraelectric (antiferroelectric) phase had an intermediate form of ordering between the crystal and isotropic amorphous phases, and it had different dynamic characteristics. Therefore, the aforementioned problem is related to the registration of two types of amorphous phases in the crystallized polymers.[83–85] According to this concept, the paraelectric (antiferroelectric) phase could have been an analogue of the rigid amorphous phase.[83–85] Thus, it is difficult to evaluate the crystallinity because the paraelectric phase could be attributed to either the amorphous domains or the crystalline phase. We evaluated two types of crystallinity with WAXS data: The Φ_1 is the crystallinity corresponding to the case in which the peak-halo is attributed to amorphous phase. The Φ_2 is the crystallinity corresponding to the case in which the peak-halo belongs to crystalline phase. Table I shows that $\phi_2 > \phi_1$. Table I also shows the fraction of the suggested paraelectric (antiferroelectric) phase ϕ_p, which depended on both the type of the copolymer and the crystallization conditions.

Table I also shows the value of *L*, which had the same values in all of VDF/TFE (94 : 6) samples and did snot depend on the crystallization conditions and phase proportion. The size of the amorphous layer (l_a) between the neighbor lamellar crystals in the stack was estimated to be $l_a = L - l_{00l}$, where l_{00l} is the longitudinal crystal size (in the direction of the macromolecule axis). l_{00l} for the β phase was estimated from the width of the 001 peak. The 001 peak was forbidden because of symmetry for the α-phase crystallization, and the longitudinal size was estimated from the width of the 002 peak. Table I shows that l_a depends on the nonpolar comonomer fraction in the VDF chain.[86] The linear crystallinity ($\phi_L = l_{00l}/L$) was also estimated. It was shown that ϕ_1, $\phi_2 > \phi_L$. This means that the crystalline phase could exist not only as stacks of lamellar crystals but also as isolated crystals in the amorphous matrix. These isolated crystals did not give an X-ray scattering maximum at small angles because they did not demote conditions for the one-dimensional diffraction.

CONCLUSIONS

The lowering of pressure during the crystallization from the melt for the VDF/TFE copolymer of 94 : 6 composition leads to the crystallization in the mixture of the metastable α modification and ferroelectric β phase. The variation of solvent affinity to the copolymer for crystallization from solution influenced the morphology of the micrometer size particles. The appearance of the peak-halo for all of the investigated copolymers indicated the presence of a paraelectric and/or antiferroelectric phase in the volume. The antiferroelectric phase in the VDF/HFP copolymer was formed by microcrystals where chains had a planar zigzag conformation. The temperature of the antiferroelectric–paraelectric transition correlated with the chain packing density in the amorphous phase. The decrease in the intramolecular dipole–dipole interaction in the studied copolymers was accompanied by an increase in the average dimensions of spaces between the neighboring lamellar crystals. It was shown by the example of the VDF/HFP copolymers that groups with high steric hindrances reduce the crystallinity and crystal dimensions and diminish the chain packing density in the amorphous phase.

References

1. The Application of Ferroelectric Polymers; Wang, T. T.; Herbert, J. M.; Glass, A. M., Eds.; Blackie: Glasgow, 1987.
2. Ferroelectric Polymers—Chemistry, Physics and Applications; Nalva, H. S., Ed.; Marcel Dekker: New York, 1995.
3. Kochervinskii, V. V. Usp Khim 1999, 68, 904.
4. Kochervinskii, V. V. Usp Khim 1994, 63, 383.
5. Galperin, E. L.; Strogalin, L. V.; Mlenik, M. P. Vysokomol Soedin 1965, 7, 933.
6. Lando, J. B.; Doll, W. W. J Macromol Sci Phys 1968, 2, 205.

7. Lando, J. B.; Doll, W. W. J Macromol Sci Phys 1968, 2, 219.
8. Doll, W. W.; Lando, J. B. J Macromol Sci Phys 1970, 4, 309.
9. Hasegawa, R.; Kobayashi, M.; Tadakoro, H. Polym J 1972, 3, 591.
10. Hasegawa, R.; Takahashi, Y.; Chatani, Y.; Tadakoro, H. Polym J 1972, 3, 600.
11. Bachmann, M. A.; Gordon, W. L.; Koenig, J. L.; Lando, J. B. J Appl Phys 1979, 50, 6106.
12. Weinhold, S.; Litt, M. H.; Lando, J. B. Macromolecules 1980, 13, 1178.
13. Bachmann, M. A.; Gordon, W. L.; Weinhold, S.; Lando, J. B. J Appl Phys 1980, 51, 5095.
14. Tashiro, K.; Kobayashi, M.; Tadakoro, H. Macromolecules 1981, 14, 1757.
15. Das-Gupta, D. K.; Doughty, K. J Appl Phys 1978, 49, 4601.
16. Das-Gupta, D. K.; Doughty, K. J Phys D 1978, 11, 2415.
17. Davis, G. T.; McKinney, J. E.; Broadhurst, M. G.; Roth, S. C. J Appl Phys 1978, 49, 4998.
18. Wang, T. T.; West, J. E. J Appl Phys 1982, 53, 6552.
19. Kochervinskii, V. V. Usp Khim 1996, 65, 936.
20. Oka, Y.; Koizumi, N. Bull Inst Chem Res Kyoto Univ 1985, 63, 192.
21. Hsu, C. C.; Geil, P. H. Polym Commun 1986, 27, 105.
22. Yang, D. C.; Chen, Y. J Mater Sci Lett 1987, 6, 599.
23. Osaki, S.; Kotaka, T. Ferroelectrics 1981, 32, 1.
24. Galperin, E. L.; Kosmyinin, B. P.; Byichkov, R. A. Vysokomol Soedin 1969, 11, 555.
25. Grubb, D. T.; Choi, K. W. J Appl Phys 1981, 52, 5908.
26. Miller, R. L.; Raisoni, J. J Polym Sci Polym Phys Ed 1976, 14, 2325.
27. Grubb, D. T.; Cebe, P.; Choi, K. W. Ferroelectrics 1984, 57, 121.
28. Gelfanbein, V.; Perlman, M. M. J Mater Sci 1983, 18, 3183.
29. Benedetti, E.; D'Alessio, A.; Bertolutti, C.; Vergamini, P.; Del Fanti, N.; Pianca, M.; Moggi, G. Polym Bull 1989, 22, 645.
30. Farmer, B. L.; Hopfinger, A. J.; Lando, J. B. J Appl Phys 1972, 43, 4293.
31. Chen, L. T.; Frank, C. W. Ferroelectrics 1984, 57, 51.
32. Lovinger, A. J.; Davis, D. D.; Cais, R. E.; Kometani, J. M. Polymer 1987, 28, 61.
33. Gregorio, R.; Cestari, M. J Polym Sci Part B: Polym Phys 1994, 32, 859.
34. Salimi, A.; Yousefi, A. A. J Appl Polym Sci 2004, 42, 3487.
35. Benz, M.; Euler, W. B.; Gregory, O. J. Langmuir 2001, 17, 239.
36. Tazaki, M.; Wada, R.; Okabe, M.; Homma, T. J Appl Polym Sci 1997, 65, 1517.
37. Kim, B. S.; Baek, S. T.; Song, K. W.; Park, I. H.; Lee, J. O.; Nemoto, N. J Macromol Sci 2004, 43, 741.
38. Kochervinskii, V. V.; Lokshin, B. V.; Palto, C. P.; Yudin, S. G. Polym Sci A 2000, 42, 245.
39. Benz, M.; Euler, W. B. J Appl Polym Sci 2003, 89, 1093.
40. Benz, M.; Euler, W. B.; Gregory, O. J. Macromolecules 2002, 35, 2682.
41. Kochervinskii, V. V.; Lokshin, B. V.; Palto, C. P.; Andreev, G. N.; Blinov, L. M.; Pethukhova, N. N. Polym Sci A (Russia) 1999, 41, 1290.
42. Chapiro, A.; Mankowski, Z.; Schmitt, N. J Polym Sci Polym Chem Ed 1982, 20, 1791.
43. Koga, K.; Nakano, N.; Hattori, T.; Ohigashi, H. J Appl Phys 1990, 67, 965.
44. Kochervinskii, V. V.; Glukhov, V. A.; Sokolov, V. G.; Romadin, V. F.; Murasheva, E. M.; Ovchinnikov, Y. K.; Trophimov, N. A.; Lokshin, B. V. Polym Sci A (Russia) 1988, 30, 2100.
45. Kochervinskii, V. V.; Murasheva, E. M. Polym Sci A (Russia) 1991, 33, 1967.
46. Kochervinskii, V. V. Polym Sci A 1998, 40, 1020.
47. Suluyanov, S. N.; Popov, A. N.; Kheiker, D. M. J Appl Crystallogr 1994, 27, 934.
48. Hashimoto, T.; Prudhomme, R. E.; Stein, R. S. J Polym Sci Part A-2: Polym Phys 1973, 11, 709.
49. Matsushige, K.; Takemura, T. J Polym Sci Polym Phys Ed 1978, 16, 921.
50. Scheinbeim, J.; Nakafuku, C.; Newman, B. A.; Pae, K. D. J Appl Phys 1979, 50, 4399.
51. Hattori, T.; Kanaoka, M.; Ohigashi, H. J Appl Phys 1996, 79, 2016.
52. Galperin, E. L.; Kosmyinin, B. P. Vysokomol Soedin 1969, 11, 1432.
53. Kochervinskii, V. V.; Kuzmin, N. N. Inorganic Materials (Russia) 1995, 31, 859.
54. Kochervinskii, V. V.; Kuzmin, N. N.; Zadorin, A. N. Polym Sci A (Russia) 1996, 38, 1188.
55. Stack, C. M.; Ting, R. T. Polym Prepr 1986, 27, 161.
56. Tajitsu, Y.; Ogura, H.; Chiba, A.; Furukawa, T. Jpn J Appl Phys 1987, 26, 554.
57. Ikeda, S.; Shimojima, Z.; Kutani, M. Ferroelectrics 1990, 109, 297.
58. Bourgaux-Leonard, C.; Legrand, J. F.; Renault, A.; Delzenne, P. Polymer 1991, 32, 597.
59. Dikshit, A. K.; Nandy, A. K. Macromolecules 2000, 33, 2616.
60. Nasef, M. M.; Suppiah, R. R.; Dahlan, K. Z. M. Solid State Ionics 2004, 171, 243.
61. Yeow, M. L.; Liu, Y. T.; Li, K. J Appl Polym Sci 2003, 90, 2130.
62. Michot, T.; Nishimoto, A.; Watanabe, M. Electrochim Acta 2000, 45, 1347.
63. Soh, Y. S.; Kim, J. H.; Gryte, C. C. Polymer 1995, 36, 3711.
64. Hong, P.-D.; Chou, C.-M.; Chuang, W.-T. J Appl Polym Sci 2001, 79, 1113.
65. Stein, R. S.; Wilkes, G. L. In Structure and Properties of Oriented Polymers; Ward, I. M., Ed.; Springer: Leeds, United Kingdom, 1975.
66. Bellet-Amalric, E. L.; Legrand, J. F. Eur Phys J 1998, 3, 225.
67. Legrand, J. F. Ferroelectrics 1989, 91, 303.
68. Flory, P. J.; Yoon, D. J.; Dill, K. Macromolecules 1984, 17, 862.
69. Zhao, H.; Wu, Z.-H.; Guo, M.-F.; Dong, B.-Z. High Energy Phys Nucl Phys 2003, 27, 1034.
70. Hahn, B. R.; Hermann-Schonher, O.; Wendorff, J. H. Polymer 1987, 28, 201.
71. Kochervinskii, B. V.; Sokolov, V. G.; Zubkov, V. M. Vysokomol Soedin A 1991, 33, 530.
72. Kochervinskii, B. V. Vysokomol Soedin A 1993, 35, 1978.
73. Takahashi, Y.; Kodama, H.; Nakamura, M.; Furukawa, T.; Date, M. Polym J 1999, 31, 263.
74. Latour, M.; Anis, K. IEEE Trans Electr Insul 1993, 28, 111.
75. Kim, K. M.; Ryu, K. S.; Kang, S.-G.; Chang, S. H,Chung, I. J. Macromol Chem Phys 2001, 202, 866.
76. Kim, K. M.; Park, N.-G.; Ryu, K. S.; Chang, S. H. Polymer 2002, 43, 3951.
77. Latour, M.; Abo Dorro, N.; Galigne, J. L. J Polym Sci Polym Phys Ed 1984, 22, 345.
78. Moggi, G.; Bonardelli, P.; Bart, J. C. J. Polym Bull 1982, 7, 115.
79. Dlubek, G.; Stejny, J.; Lupke, T.; Bamford, D.; Petters, K.; Hubner, C.; Alam, M. A.; Hill, M. J. J Polym Sci Part B: Polym Phys 2002, 40, 65.
80. Kochervinskii, V. V.; Malyshkina, I. A.; Markin, G. V.; Gavrilova, N. D.; Bessonova, N. P. J Appl Polym Sci 2007, 105, 1101.
81. Tashiro, K.; Takano, M.; Kobayashi, M.; Chatani, Y.; Tadokoro, H. Ferroelectrics 1984, 57, 297.
82. Xu, Y.; Mackenzie, J. D. J Non-Cryst Solids 1999, 246, 136.
83. Xu, H.; Cebe, P. Macromolecules 2004, 37, 2797.
84. Huo, P.; Cebe, P. Macromolecules 1992, 25, 902.
85. Huo, P.; Cebe, P. J Polym Sci Part B: Polym Phys 1992, 30, 239.
86. Kochervinskii, V. V.; Volkov, V. V.; Dembo, K. A. Phys Solid State (Russia) 2006, 48, 1083.